**CSIRO** PUBLISHING

**Full Papers**

www.publish.csiro.au/journals/ajc

*Aust. J. Chem.* **2003**, *56*, 1051–1057

# Size Effects in ZnO: The Cluster to Quantum Dot Transition

*Annabel Wood*,[A] *Michael Giersig*,[B] *Michael Hilgendorff*,[B] *Antonio Vilas-Campos*,[C] *Luis M. Liz-Marzán*[C] *and Paul Mulvaney*[A,D,E]

[A] Chemistry School, University of Melbourne, Parkville 3010, Australia.
[B] Center of Advanced European Studies and Research (CAESAR), Bonn 53175, Germany.
[C] Departamento de Química Física, Universidade de Vigo, Vigo 36200, Spain.
[D] Max Planck Institute for Colloids and Surfaces, Golm 14476, Germany.
[E] Author to whom correspondence should be addressed (e-mail: mulvaney@unimelb.edu.au).

The use of tetraalkylammonium hydroxides to prepare ZnO colloids with diameters ranging from 1 to 6 nm is described. The position of the first excitonic transition has been measured by UV-vis spectrometry and correlated with the particle size, which has been measured using high-resolution transmission electron microscopy (HRTEM), X-ray diffraction (XRD), and ultracentrifugation (UC). The exciton transition is first visible at 265–270 nm corresponding to particle diameters around 1 nm; the exciton absorption band then becomes sharper and narrower, while the band red-shifts only slowly. Based on the sizing data from HRTEM, XRD, and UC, it is concluded that the quantum size effect at sizes less than the Bohr radius is significantly less than predicted from the Kayanuma equation. Based on the blue-shift in the trap emission as a function of nanocrystal size, the effective masses of the electron and hole ($m_e$, $m_h$) remain constant in particles down to 1 nm in diameter, with a relative value given by $m_e/(m_e + m_h) = 0.55 \pm 0.04$.

Manuscript received: 12 May 2003.
Final version: 22 July 2003.

Nucleation of nanocrystals has long been one of the most difficult processes to monitor directly except through fast kinetic spectroscopy. To date, pulse radiolysis has been perhaps the most successful tool for direct observation of colloid nucleation. The initial steps in the formation of Ag,[2] AgI,[3] and CdS[4] particles have all been examined using transient spectrophotometry coupled with radiation-induced nucleation. While these studies have demonstrated that the absorption spectra of all nuclei and clusters are strongly size dependent, the short lifetime of these species has made it difficult to directly correlate the spectral properties of species with their size. This information is important for establishing the size regime in which the electronic structure evolves from having a molecular character to completely delocalized orbitals, interpretable using band theory. Generally, the effective mass approximation appears to hold down to sizes under the Bohr radius.[5,6]

In this paper, an extremely simple method for the preparation of ZnO clusters ranging in size from 1 to 6 nm is described using tetraalkylammonium hydroxides as the precursor. This allows extremely high degrees of supersaturation to be achieved, which are not possible with NaOH and LiOH due to their low solubility in ethanol. Surprisingly the nucleation and growth of the clusters is still found to take place over minutes rather than milliseconds and permits the synthesis of smaller ZnO particles than has been previously possible. The ease of preparation prompted us to search for the size regime in which ZnO undergoes a transition from molecular to semiconducting properties.

## Experimental

### *ZnO Quantum Dot (QD) Preparation*

50 mL of 20 mM $Zn(OAc)_2 \cdot 2H_2O$ (Aldrich) in absolute ethanol was placed in a water-jacketed reaction vessel. The solution was then heated or cooled to the desired temperature. For smaller particles, temperatures around 0°C are optimal. 0.85 mL of tetramethylammonium hydroxide (TMAOH; 25 wt-% in methanol) was then injected through a microsyringe using a stepper motor to maintain a constant injection rate of 0.05 mL $min^{-1}$. ZnO colloids also formed when rapid injection was used, but this was less reproducible. If lower concentrations were employed, nucleation often did not take place, and the solution contained only non-luminescent clusters. Samples were prepared for TEM on carbon coated copper grids (30 Å film thickness).

### *Characterization*

The particles were examined using both a JEOL 4000EX microscope operating at 400 kV and a Philips CM12 at 120 kV. The zeta-potential of freshly prepared 1 mM ZnO QD solutions with no adjustment to the ionic strength was determined to be +10 mV using laser Doppler electrophoresis. This implies superequivalent adsorption of the alkylammonium cations, but the low potential means weak resistance to flocculation. Time-resolved spectra were collected with a diode array spectrophotometer (HP8453, Hewlett–Packard). Fluorescence spectra were recorded on a fluorimeter (Eclipse, Cary) with excitation at 260, 280, or 300 nm depending on particle size. Particle sizing of the QDs was carried out using an analytical ultracentrifuge (Optima XL-I, Beckman) equipped with scanning absorption optics (200–800 nm,

 10.1071/CH03120 0004-9425/03/101051

accuracy ±2 nm) operating at 30 000–60 000 rpm, and could record spectra versus time in the centrifuge cell at different cell depths. The software corrects the measured light intensity using an identical reference cell containing ethanol. Typically 3 mL of sol was centrifuged with an absorbance around 1 $cm^{-1}$. The samples were generally maintained at 4 and 9°C. The ZnO bulk density of 5.6 g $cm^{-3}$ for all samples was assumed in calculating the particle size. The viscosity of ethanol at different temperatures was calculated by interpolation of literature data[7] using the form $\eta[\text{mPa s}] = \alpha T[^\circ\text{C}]^{-\beta}$, with the best fit being found for $\alpha = 12$ and $\beta = 0.567$.

## Results

Using the protocol outlined above, it was found that ZnO colloids with sizes between about 1 and 6 nm could be readily prepared with a 10–15% size distribution. The UV-vis absorption and fluorescence spectra of these particles are shown in Figure 1*a* as a function of the preparation temperature. The smallest particles displayed an exciton resonance at 265 nm, a shorter wavelength than other preparations have yielded to date. Larger particles with absorption peaks around 355 nm were formed by ageing, and this value approaches the bulk ZnO exciton wavelength.[8] The optimal ratio of TMAOH/Zn was found to be about 1.6–2.0 : 1, based on the sharpness of the exciton band (Fig. 1*b*). Several solvents were also tested. In methanol, the nucleation of ZnO often did not take place due to the higher dielectric constant and solubility of ZnO, while in longer aliphatic alcohols, it was difficult to dissolve the $Zn(OAc)_2$. It was also found that better results were obtained when TMAOH was added to $Zn(OAc)_2$, rather than vice versa. Fresh dry ethanol yielded the best results, while water was deleterious for small particle formation.

It was observed that the visible trap luminescence varied from blue to green to yellow as the particles grew. This indicates that the process leading to trap emission involves a quantized charge carrier in one of the bands. In Figure 1*c*, both the full-width at half-maximum (FWHM) of the trap emission and the peak trap emission energy are plotted as a function of the exciton energy. The plot of trap emission energy versus exciton energy is quite linear with a slope of 0.55 ± 0.04. The FWHM of the trap emission is a little scattered but is basically independent of particle size for QDs with diameters down to 1 nm.

High resolution TEM images of a number of ZnO QDs are shown in Figure 2. All the ZnO particles observed by HRTEM were crystalline though the morphology varied considerably, and all particles could be unambiguously indexed to wurtzite. A very weak dependence of the lattice spacing on particle size was found from Fourier analysis of the lattice planes, with the smallest particles having a slightly larger lattice plane spacing of 0.26 nm compared with 0.24 nm. The smallest particles were difficult to size reliably, while agglomeration of the particles and growth due to Ostwald ripening also made XRD sizing of smaller particles difficult. It was found that by ageing the 0.01 M ZnO samples for 24 h in 0.020 M tetraethylorthosilicate (TEOS), which was added dropwise to the colloid at 5°C, a thin shell of hydrated and amorphous silica built up on the ZnO surface, which prevented particle growth. Such sols were noticeably less sensitive to water addition, and could be rotary evaporated to dryness. The particle

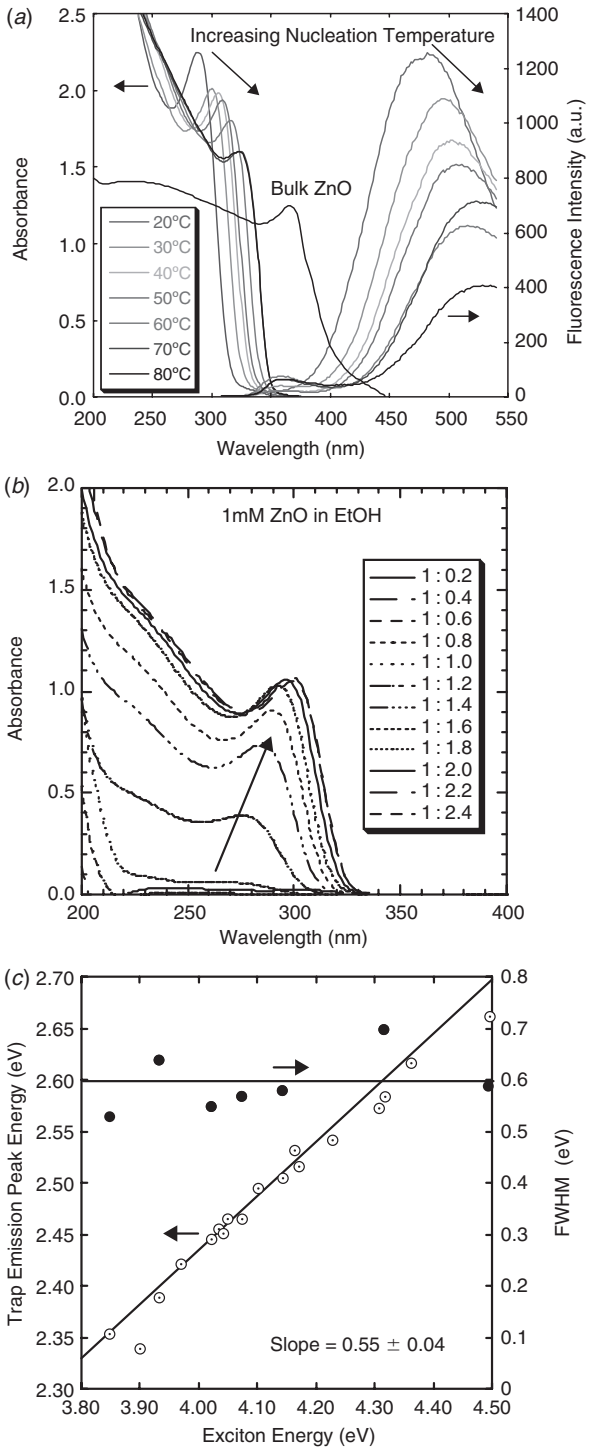


**Fig. 1.** (*a*) UV-visible absorption spectra of ZnO QDs prepared at various temperatures, and their luminescence spectra ($\lambda_{exc}$ 280 nm). (*b*) Titration of zinc acetate dihydrate (10 mM) in dry 99.5% ethanol with successive aliquots of TMAOH (0.842 mL) at room temperature. Measurements of the absorption spectra were performed using a 2 mm cell. Ageing experiments revealed a Zn/TMAOH ratio of 1 : 1.6 provided the most stable ZnO QDs. (*c*) The peak trap emission energy (⊙) and its FWHM (●) as a function of the exciton energy.[48] [ZnO] = 1 mM; solvent ethanol; [TMAOH] = 1.6 mM.

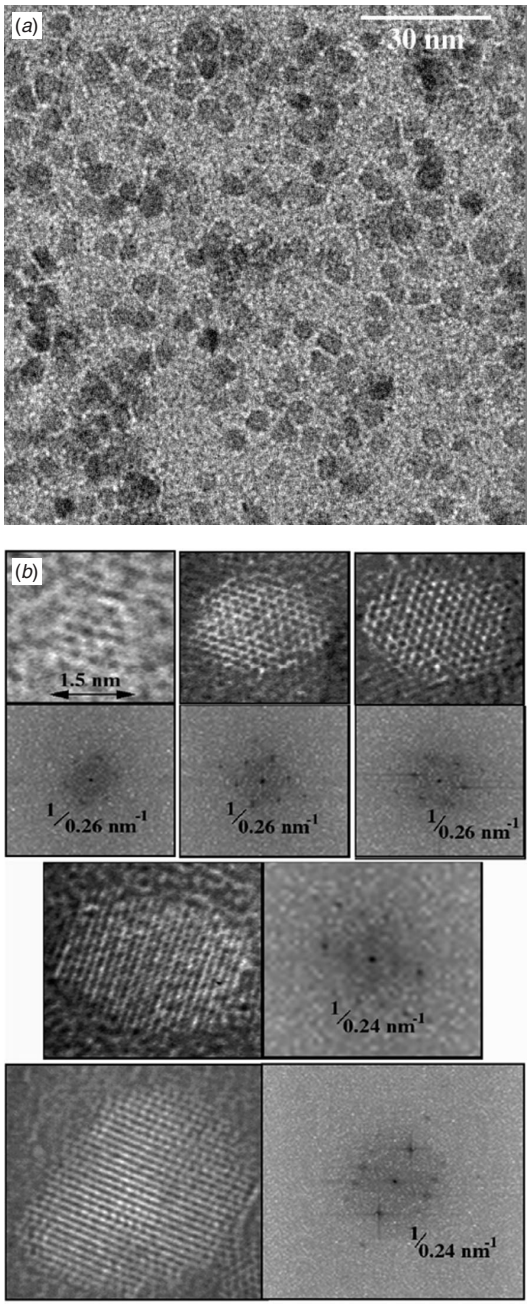


**Fig. 2.** (*a*) Electron micrographs of 4 nm ZnO particles showing particle morphology and size distribution. (*b*) 400 kV TEM gallery of individual particles from QD samples prepared at different temperatures, showing lattice planes. The power spectrum indicates that all crystallites possess the wurtzite structure.

sizes in these blue-luminescing, silica-capped ZnO powders were determined by Rietveld refinement of the XRD powder spectra (see the Accessory Materials). Wurtzite was the only phase found by XRD.

Ultracentrifugation was employed to size the ZnO QDs less than 6 nm in diameter. This has previously been used successfully by Cölfen et al. to size ZnO clusters and Pt particles.[9,10] In Figure 3, a typical gallery of size

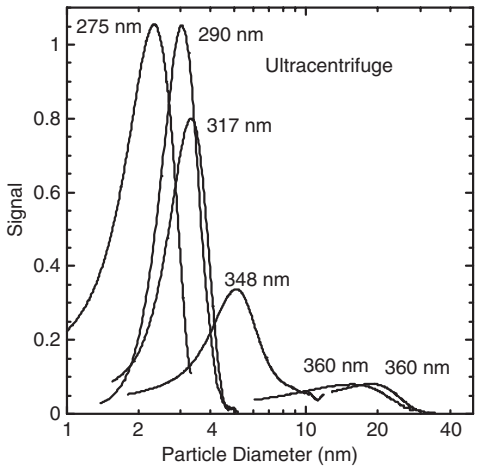


**Fig. 3.** Typical size distributions of different samples of ZnO QDs, obtained from ultracentrifugation. Numbers indicate the measured $\lambda_{max}$.

distributions calculated from ultracentrifugation is presented. All samples were measured within 20 min of preparation. Once cooled within the UC, growth was extremely slow. The actual exciton peak position of the sample is indicated. Note that larger colloids have broader distributions, which indicates that there is coagulation occurring during synthesis at higher temperatures. However we attribute the narrow size distributions at smaller diameters to Ostwald ripening. The reasons for this are several. Firstly, we find that the red-shift in the absorption spectrum upon ageing is insensitive to colloid concentration, which is inconsistent with particle aggregation of the smallest QDs. Secondly, dimerization should lead to much stronger 'quantized' spectral shifts, rather than the gradual ones we observe by titration or ageing (Fig. 1*b*). Finally, the spectra sharpen during the early phases of growth immediately after nucleation and subsequently broaden. We believe this latter phase marks the onset of coagulation. Nevertheless there is evidence for particle aggregation from earlier studies, and we cannot exclude that 'quantized aggregation' is possible.[11]

The ZnO nucleation process was monitored using a diode array spectrophotometer. In Figure 4, we show the time-resolved spectra obtained from mixing $Zn(OAc)_2$ and TMAOH at 25°C. Immediately after mixing, there was an initial intense absorption band present that peaked around 210 nm. This band is the charge transfer to solvent band of $OH^-_{(aq)}$. Within 1 min a shoulder could be resolved at 230 nm, thereafter a weak plateau formed, extending to around 250 nm. This band grew in intensity and the exciton absorption band emerged at about 265 nm, but during the early stages as the absorption band increased, the band only slightly red-shifted. Data collected at 10°C appeared identical although the growth rate was strongly retarded.

In Figure 5, we have collated the literature data for the exciton band positions of ZnO QDs as a function of size. Some authors have measured either the FWHM of the exciton peak or the extrapolated wavelength onset. We have not included these data, but have focussed on those where the size and a true peak position have both been independently

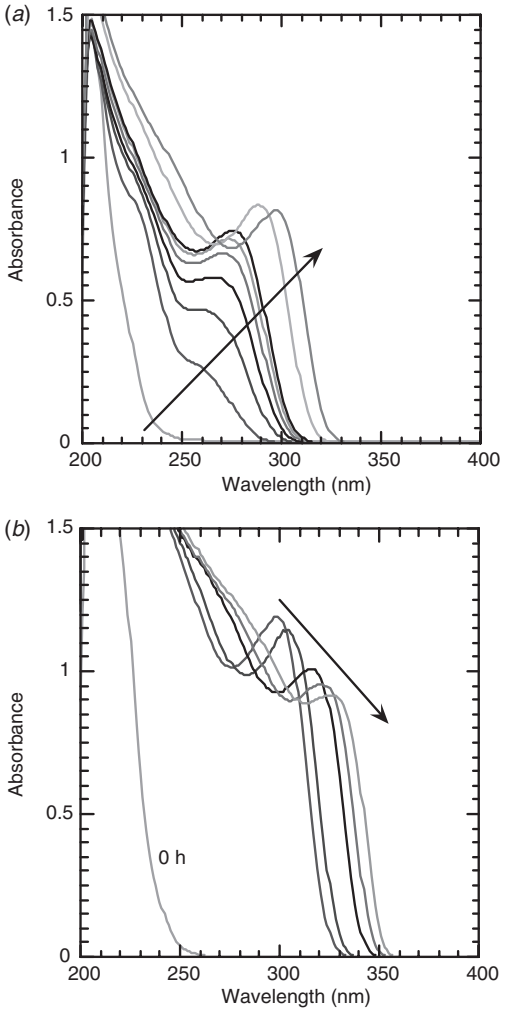


**Fig. 4.** Evolution of the absorbance spectra of 1 mM ZnO QDs at 25°C, measured over (*a*) 15 min and (*b*) 20 h.

measured. We have added in our own HRTEM, UC, and XRD data, which extend down to particle diameters of just 1 nm. The result is a fairly consistent set of data for ZnO QDs.

## Discussion

There have been numerous papers over the last 15 years on the growth of ZnO QDs and their emission properties.[12–32] Most researchers have employed the synthesis described by Spanhel and Anderson,[33] which is quite time consuming and involves several steps. The protocol described here requires just a few minutes and obviates the long distillation process needed in this earlier preparation and also circumvents the solubility problems associated with the use of NaOH and LiOH. The use of organic bases for ZnO synthesis has not been explored to date and enables the rapid preparation of ZnO QDs with a range of sizes.

### *Particle Sizing*

The TEM and XRD data indicate that all the ZnO particles consist of crystalline wurtzite. The smallest particles

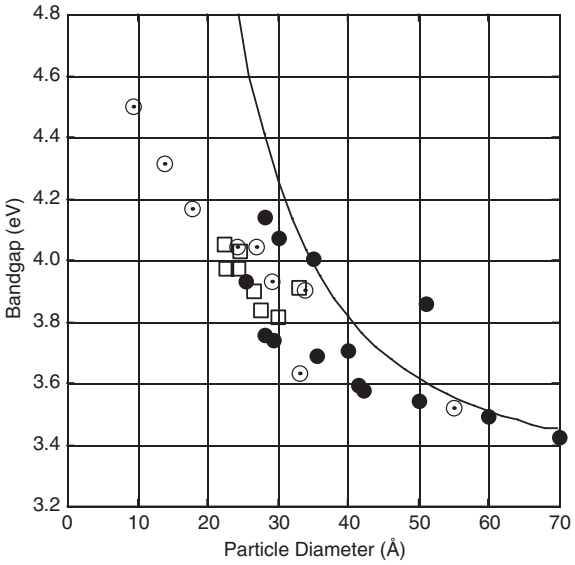


**Fig. 5.** Plot of literature and current data for the exciton energy in ZnO particles versus size. The line of best fit to the majority of the data is given by the Kayanuma equation with an exciton radius of 2.4 nm and a binding energy of 30 meV. ⊙: XRD results; □: UC results; ●: literature data.

for which lattice planes could be discerned were around 0.9–1.1 nm at 400 kV. In addition, there is evidence for only a very small shift in the lattice parameters at the smallest particle sizes, and consequently the density of ZnO is not significantly altered down to around 1 nm in diameter. The extraction of lattice parameters from the power spectrum is not sufficiently accurate to allow a plot of lattice parameter versus size; we can only state that there is a discernible increase for the smallest particles. We believe that, provided the particles retain the bulk ZnO density, UC offers the most accurate sizing method for ultrasmall ZnO QDs, since the major source of error in such measurements with nanocrystals is the particle density. In principle, a further limitation of UC sizing of nanoparticles is calculation of the sedimentation potential which, at low ionic strength and high zeta-potential, leads to a systematic underestimation of the particle radius.[1] However, for our colloids with an ionic strength of 0.01 and a zeta-potential of less than 10 mV, we calculate that the introduced error is maximally 5–10%. It was also found that as long as fresh colloids and low UC temperatures were used, coalescence during sizing was not a problem.

### *Quantized Trap Emission*

While there is considerable uncertainty over the process responsible for the trap emission, it is generally concluded that it is either the reaction of trapped holes with free conduction band electrons or, conversely, the recombination of trapped electrons with free valence band holes. The role of a trapped carrier is evident from the fact that the emission is strongly red-shifted from the exciton energy, and from the fact that the half-life for the trap emission is typically 0.5–3 μs, several thousand times slower than the radiative recombination rate for excitons in bulk ZnO.[8,25] The role of a free

**Table 1. Dielectric data for ZnO**

| Parameter | Value and reference | Comments |
|---|---|---|
| Reduced mass of electron $m_e^*$ | 0.24[14,43,44]; 0.28[8]; 0.28[45]; 0.24[46] | |
| Reduced mass of hole $m_h^*$ | 0.45[14,43,44]; 0.59[8]; 0.50[45]; 0.45[46] | |
| Exciton binding energy $R$ [meV] | 59[45] | |
| Bulk dielectric constant $\varepsilon_r$ | 3.7[43,44] | |
| Bulk refractive index at 632 nm | 1.92[14] | |
| Zero-frequency dielectric constant | $\varepsilon_0^{\parallel} = 8.8 \pm 0.4$; $\varepsilon_0^{\perp} = 7.8 \pm 0.3$[8] | Measured using IR spectroscopy |
| Static dielectric constant | $\varepsilon^{\parallel} = 11$; $\varepsilon^{\perp} = 8.5$[8] | Measured at radio frequencies |
| Static relative permittivity $\varepsilon_{st}$ | 6.51[8] | |
| Exciton radius | 13[47]; 18[8]; 25[46] | |
| Exciton radius | 28.7 | Calculated using $h^2\varepsilon_r\varepsilon_0/\mu\pi e^2$ |

carrier is also equally clear from the fact that the ZnO QD emission blue shifts with decreasing particle size (Fig. 1*c*). Since the FWHM of the emission is hardly altered with particle size (see Fig. 1*c*), this implies that the surface states do not interact strongly with the band energy levels; that is, they are strongly localized surface states.

Since only one carrier is involved, the shift in the energy of the trap emission with particle radius is less than the shift in the exciton absorption. The relative shift of the trap emission relative to the exciton band shift is given approximately by[17]

$$\frac{\Delta E_{tr}(e,h)}{\Delta E_{exc}} \approx \frac{m_{e,h}^{-1}}{m_e^{-1} + m_h^{-1}} \qquad (1)$$

where e and h refers to the appropriate charge carrier involved in the emission process. Since the effective masses of the electron and hole are 0.24 and 0.45 respectively (Table 1), the relative values of the slope are 0.65 and 0.35 respectively, depending on which carrier is involved. The good fit in Figure 1*c* with a slope of 0.55, supports the assignment of trap emission in ZnO to the reaction of free conduction band electrons with trapped holes. Inclusion of the electron–hole Coulomb interaction would improve the agreement. This interpretation is in accord with the results of Meulenkamp and coworkers on the kinetics of trap emission.[19–21] They postulated that free valence-band holes are trapped on singly ionized oxygen vacancies ($V_O^+$), and that electron capture by the resultant doubly ionized site ($V_O^{++}$) results in the trap emission

$$V_O^+ + h^+ \longrightarrow V_O^{++} \qquad (2)$$

$$e^- + V_O^{++} \longrightarrow V_O^+ + h\nu \qquad (3)$$

It is assumed by most workers that the first electron within the neutral vacancy is a very shallow donor. An important corollary of this interpretation is that the effective masses of electrons and holes in ZnO QDs remain close to their respective bulk values down to particle sizes of just 1 nm, and we conclude that over this range of sizes $m_e/(m_e + m_h) = 0.55 \pm 0.04$.

*Exciton Position in ZnO QDs*

From Table 1, it can be seen that despite a large number of studies there is still some uncertainty in the values of the static dielectric constant and the effective mass of the charge carriers in ZnO. Depending on the values chosen, the Bohr radius $a_B$ is predicted to lie between 15 and 30 Å, with the exciton binding energy varying from about 30–160 meV. A Bohr radius of about 24 Å and a binding energy of 30 meV are close to representative, and are consistent with the effective masses predicted from the trap emission data in the previous section. Most of the ZnO clusters lie within the strong confinement regime, but fits to the exciton energy $E$, in terms of bulk band gap $Eg$ and the Rydberg energy $Ry$, using the Kayanuma relation, Equation (*4*), are poor, as is evident from Figure 5.[34]

$$E = Eg + \pi^2 \left(\frac{a_B}{a}\right)^2 Ry - 1.786\frac{a_B}{a}Ry - 0.248Ry \qquad (4)$$

The fit depends only weakly on the parameters chosen from Table 1, and the introduction of a finite wall potential of 7.8 eV (based on a band gap of 4.4 eV and an ionization energy of 3.4 eV) only improves the fits marginally. We conclude that for small ZnO QDs, the exciton shift is not as pronounced as expected from the Brus or Kayanuma equations.

*Nucleation Kinetics*

A key finding of this work is that the rate of growth of ZnO formed from TMAOH and $Zn(OAc)_2$ is remarkably slow and strongly temperature dependent, and the kinetics of growth can be easily followed spectrophotometrically. This result was unexpected, since the high solubility of TMAOH compared with LiOH results in very high degrees of supersaturation. This sluggish growth suggests that condensation of clusters and/or the desorption of acetate ligands restricts growth of the clusters, as previously postulated by several groups.[35,36] Since we can monitor the growth of the particles from the moment of titration and we see no absorption or emission from species below 265 nm (Fig. 4), we propose that the ZnO QDs with an absorption transition at 265 nm are the smallest clusters displaying 'delocalized' charge carriers. From the UC and XRD data, these particles are 1 nm in diameter. Note that during the growth and slow red-shift of the band at 265 nm in Figure 4 at 25°C, the absorption at shorter wavelengths (200–250 nm) does not rise proportionally. For example, at 230 nm, there is an increase from 0.8 to 1.2, while at 265 nm the absorbance rises by a factor of four from 0.2 to 0.8. This implies that the absorption is not simply due to the continuous nucleation of fresh particles of a distinct size. The creation of an increasing number of identically sized clusters would lead to a proportional increase across the spectrum, i.e.

Beer's Law would be obeyed. Instead we believe the spectra reflect the accumulation of monomers onto the clusters, or the dissolution of unstable clusters onto stable nuclei.

There are few data on the optical properties of ZnO multinuclear clusters. However it has been shown by Kunkeley and Vogler[37] that the tetramer $[Zn_4O(OAc)_6]$ has an absorbance peak at 216 nm ($\varepsilon$ 62 200 $M^{-1}$ $cm^{-1}$), which would be difficult to observe under the intense $OH^-_{(aq)}$ CTTS band at 210 nm. This species is not stable in water, where it hydrolyzes. Dimerization of this species could generate the initial ZnO QDs, with particle nucleation controlled by the hydrolysis or desorption of these multidentate acetate groups and bridging of the hydroxy clusters. Since no bleaching is observed between 220 and 270 nm as the exciton band grows, the precursors to the QDs absorbing at 265 nm are only weakly absorbing from 220–270 nm, consistent with nucleation from $[Zn_4O(OAc)_6]$. This species has been proposed as the active cluster in ZnO growth by several groups.[35,36,38,39]

*Clusters versus Nanocrystals*

ZnO synthesis at −5°C often resulted in no QD formation, just bands between 200 and 240 nm. When such solutions were aged, the absorption band at 240 nm slowly broadened to become a very weak shoulder that extended out to 355 nm over a period of hours or days. Under these conditions, a small number of large ZnO particles resulted. This clearly indicates that nucleation is an activation controlled process. Following injection of TMAOH, Zn ions are converted into $[Zn_4O(OAc)_6]$ or other oligomers, which are only metastable and are non-absorbing at 265 nm. At very low temperatures, growth, Ostwald ripening, and aggregation are all retarded, but so is the rate of nucleation. A supersaturated solution of $[Zn_4O(OAc)_6]$ or other oligomers results.[14,35,36,40,41] Random, slow nucleation in such solutions results in a few larger ZnO particles forming over a period of hours. Conversely, at temperatures between 5 and 25°C, and in the presence of sufficient TMAOH, the oligomers hydrolyze to create a large number of ZnO QDs with a critical size of about 1 nm, corresponding to the highest energy at which a distinct exciton transition is observed. The optical transitions in Figure 1*b* during TMAOH titration result from rapid accretion of the excess $[Zn_4O(OAc)_6]$ onto these nuclei. Accretion of monomers leads to slow size increases until the electrostatic double layer interaction stabilizes the particles at about 1.5–2.0 nm. As monomers or tetramers add onto the proto-QD, the cluster size barely increases, but there is a dramatic increase in the oscillator strength. This may reflect the increasing delocalization of the electron and hole.

Though the synthesis of ZnO QDs using TMAOH is extremely simple, optimizing the process of ZnO formation is not trivial. There is an optimal temperature for formation of a narrow population of small particles. This is a compromise that involves minimizing the aggregation of nuclei at high temperature due to the low zeta-potential and maximizing the rate of nucleation from the solution of oligomers that forms following TMAOH injection, since very low temperatures (<−5°C) completely inhibit nucleation of stable clusters. Colloid aggregation between nuclei slows down, even at constant zeta-potential, since the interaction energy increases rapidly with particle size. Cölfen et al. have previously demonstrated by ultracentrifugation that the growth of Pt and ZnO may be controlled by magic-number aggregation kinetics.[9,10] They proposed that only the addition of pyramidal clusters of $(ZnO)_4$ units produces stabilized clusters. Hilgendorff et al. have likewise proposed that pyramidal ZnO clusters play a key role in colloid formation.[42]

In summary, by monitoring the absorption changes during the titration of Zn ions to form ZnO, we believe that a concentrated cluster solution forms, which does not possess semiconductor-like absorption spectra. The 'quantized coalescence' of this species produces the first ZnO QDs with exciton bands at 265 nm. A diameter of 1 nm corresponds to an aggregation number of about 18, perhaps four $[Zn_4O(OAc)_6]$ clusters. The kinetics of formation of the 265 nm species is strongly dependent on supersaturation and temperature. Slow addition of clusters or monomeric Zn to the 265 nm species and Ostwald ripening cause the band to increase in intensity, with a maximum oscillator strength occurring when the exciton band lies at 290 nm.

## Conclusions

Using a simplified colloid synthesis route, we have prepared and sized ZnO colloids down to 1 nm in diameter using HRTEM and UC. The size distributions broaden with ageing as expected if some growth occurs by coagulation. However our inability to completely prevent ripening in a variety of solvents or at lower temperatures suggest that for the smallest particles, Ostwald ripening is the primary mechanism as proposed by Meulenkamp. The 'nucleation spectroscopy' data suggest that the exciton oscillator strength grows rapidly around a radius of 0.5 nm, which is about one-quarter of the estimated Bohr radius. The shift in trap emission with particle size is consistent with recombination by a trapped hole and a free conduction electron, and this data independently support a constant effective mass for both electron and hole down to ZnO sizes less than the Bohr radius. Fourier analysis of the HRTEM images suggest that the density of ZnO is close to bulk values down to around 1 nm in size.

## Accessory Materials

Accessory materials for this paper are available, until October 2008, from the *Australian Journal of Chemistry* or from the authors.

## Acknowledgments

A.W. thanks the University of Melbourne for a postgraduate scholarship. P.M. thanks Markus Antonietti for his support and the Humboldt Foundation for facilitating this research through the award of a Humboldt Fellowship; Helmut Cölfen and Antje Völkel at the Max Planck Institute in Golm are also acknowledged for their invaluable assistance with the UC experiments. This research was supported by ARC grant A29930217. David Broido's calculation of the finite potential well energy levels is appreciated.

## References


[1] R. O'Brien, L. R. White, *J. Chem. Soc., Faraday Trans. 2* **1978**, *74*, 1607.
[2] P. Mulvaney, A. Henglein, *J. Phys. Chem.* **1990**, *94*, 4182.
[3] K. H. Schmidt, R. Patel, D. Meisel, *J. Am. Chem. Soc.* **1988**, *110*, 4882.
[4] V. Swayambunathan, D. Hayes, K. Schmidt, Y. Liao, D. Meisel, *J. Am. Chem. Soc.* **1990**, *112*, 3831.
[5] S. V. Gaponenko, *Optical Properties of Semiconductor Nanocrystals* **1998** (Cambridge University Press: Cambridge).
[6] L. Brus, *J. Phys. Chem.* **1986**, *90*, 2555.
[7] D. R. E. Lide, *CRC Handbook of Chemistry and Physics*, *80th ed.* **1999** (CRC Press: Boca Raton, FL).
[8] W. Hirschwald, P. Bonasewicz, L. Ernst, M. Grade, D. Hofmann, S. Krebs, R. Littbarski, G. Neumann, M. Grunze, D. Kolb, H. J. Schulz, *Zinc Oxide*: *Properties and Behaviour of the Bulk*, *the Solid/Vacuum*, *and Solid/Gas Interface* **1981**, Vol. 7 (North-Holland: Amsterdam).
[9] H. Cölfen, T. Pauck, *Colloid Polym. Sci.* **1997**, *275*, 175.
[10] H. Cölfen, T. Pauck, M. Antonietti, *Progr. Colloid Polym. Sci.* **1997**, *107*, 136.
[11] M. Kohls, T. Schmidt, H. Katschorek, L. Spanhel, G. Muller, N. Mais, A. Wolf, A. Forchel, *Adv. Mater.* **1999**, *11*, 288.
[12] M. Haase, H. Weller, A. Henglein, *J. Phys. Chem.* **1988**, *92*, 482.
[13] D. W. Bahnemann, C. Kormann, M. R. Hoffmann, *J. Phys. Chem.* **1987**, *91*, 3789.
[14] E. M. Wong, J. E. Bonevich, P. C. Searson, *J. Phys. Chem. B* **1998**, *102*, 7770.
[15] E. M. Wong, P. C. Searson, *Chem. Mater.* **1999**, *11*, 1959.
[16] A. van Dijken, E. A. Meulenkamp, D. Vanmaekelbergh, A. Meijerink, *J. Phys. Chem. B* **2000**, *104*, 4355.
[17] A. van Dijken, E. A. Meulenkamp, D. Vanmaekelbergh, A. Meijerink, *J. Lumin.* **2000**, *90*, 123.
[18] A. van Dijken, E. A. Meulenkamp, D. Vanmaekelbergh, A. Meijerink, *J. Lumin.* **2000**, *87/89*, 454.
[19] A. van Dijken, E. A. Meulenkamp, D. Vanmaekelbergh, A. Meijerink, *J. Phys. Chem. B* **2000**, *104*, 1715.
[20] K. Vanheusden, C. H. Seager, W. L. Warren, D. R. Tallant, J. Caruso, M. J. Hampden-Smith, T. T. Kodas, *J. Lumin.* **1997**, *75*, 11.
[21] K. Vanheusden, W. L. Warren, C. H. Seager, D. R. Tallant, J. A. Voigt, B. E. Gnade, *J. Appl. Phys.* **1996**, *79*, 7983.
[22] P. E. de Jongh, E. A. Meulenkamp, D. Vanmaekelbergh, J. J. Kelly, *J. Phys. Chem. B* **2000**, *104*, 7686.
[23] S. Chen, U. Nickel, X. Ren, *J. Colloid Interface Sci.* **1995**, *176*, 286.
[24] S. Chen, U. Nickel, *J. Chem. Soc., Chem. Commun.* **1996**, 133.
[25] E. A. Meulenkamp, *J. Phys. Chem. B* **1998**, *102*, 5566.
[26] E. A. Meulenkamp, *J. Phys. Chem. B* **1998**, *102*, 7764.
[27] E. A. Meulenkamp, *J. Phys. Chem. B* **1999**, *103*, 7831.
[28] P. V. Kamat, B. Patrick, *J. Phys. Chem.* **1992**, *96*, 6829.
[29] P. V. Kamat, I. Bedja, S. Hotchandani, L. K. Patterson, *J. Phys. Chem.* **1996**, *100*, 4900.
[30] P. Hoyer, R. Eichberger, H. Weller, *Ber. Bunsenges. Phys. Chem.* **1993**, *97*, 630.
[31] P. Hoyer, H. Weller, *Chem. Phys. Lett.* **1994**, *221*, 379.
[32] P. Hoyer, H. Weller, *J. Phys. Chem.* **1995**, *99*, 14096.
[33] L. Spanhel, M. A. Anderson, *J. Am. Chem. Soc.* **1991**, *113*, 2826.
[34] Y. Kayanuma, *Phys. Rev. B* **1988**, *38*, 9797.
[35] M. S. Tokumoto, S. H. Pulcinelli, C. V. Santilli, V. Briois, *J. Phys. Chem. B* **2003**, *107*, 568.
[36] M. S. Tokumoto, S. H. Pulcinelli, C. V. Santilli, A. F. Craievich, *J. Non-Cryst. Solids* **1999**, *247*, 176.
[37] H. Kunkeley, A. Vogler, *Chem. Comm.* **1990**, 1204.
[38] M. Hilgendorff, L. Spanhel, C. Rothenhausler, G. Muller, *J. Electrochem. Soc.* **1998**, *145*, 3632.
[39] Y. Inubushi, R. Takami, M. Iwasaki, H. Tada, S. Ito, *J. Colloid Interface Sci.* **1998**, *200*, 220.
[40] M. Kohls, T. Schmidt, H. Katschorek, L. Spanhel, G. Muller, N. Mais, A. Wolf, A. Forchel, *Adv. Mater.* **1999**, *11*, 288.
[41] T. Schmidt, G. Muller, L. Spanhel, *Chem. Mater.* **1998**, *10*, 65.
[42] M. Hilgendorff, L. Spanhel, C. Rothenhausler, G. Muller, *J. Electrochem. Soc.* **1998**, *145*, 3632.
[43] L. E. Brus, *J. Chem. Phys.* **1983**, *79*, 5566.
[44] L. E. Brus, *Nanostruct. Mater.* **1992**, *1*, 71.
[45] *Landolt-Börnstein Numerical Data and Functional Relationships in Science and Technology* (Ed. O. Madelung) **1988**, Vol. III-17 (Springer: Berlin).
[46] G. Redmond, A. O'Keeffe, C. Burgess, C. MacHale, D. Fitzmaurice, *J. Phys. Chem.* **1993**, *97*, 11 081.
[47] B. Enright, D. Fitzmaurice, *J. Phys. Chem.* **1996**, *100*, 1027.
[48] R. E. Dietz, J. J. Hopfield, D. G. Thomas, *J. Appl. Phys.* **1961**, *32 (suppl)*, 2282.

10.1071/CH03120_AC

Accessory Publication: *Aust. J. Chem.*, 2003, **56**(10), 1051–1057.

## Accessory Material

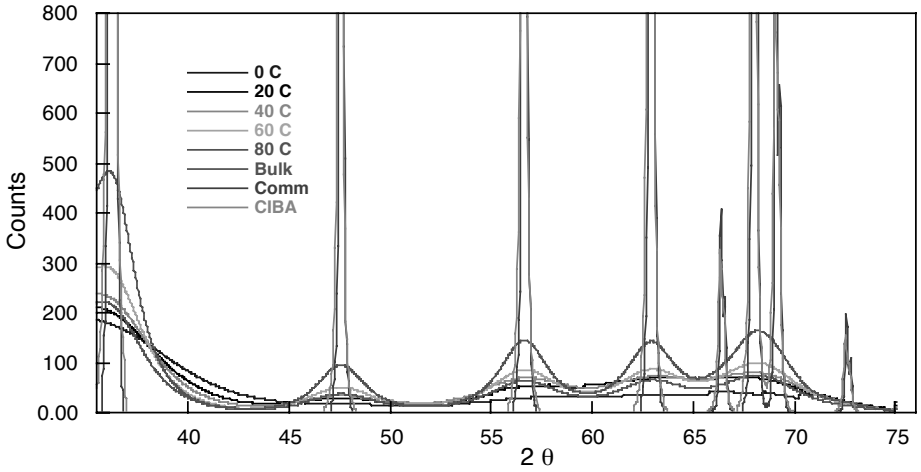


*Fig. 1*: X-ray diffraction patterns for samples of Q-ZnO between 0 and 80°C, and also heated to resemble bulk ZnO. A commercially obtained sample (Comm) is included for comparison. Note the broadening of the peaks of the Q-ZnO samples.

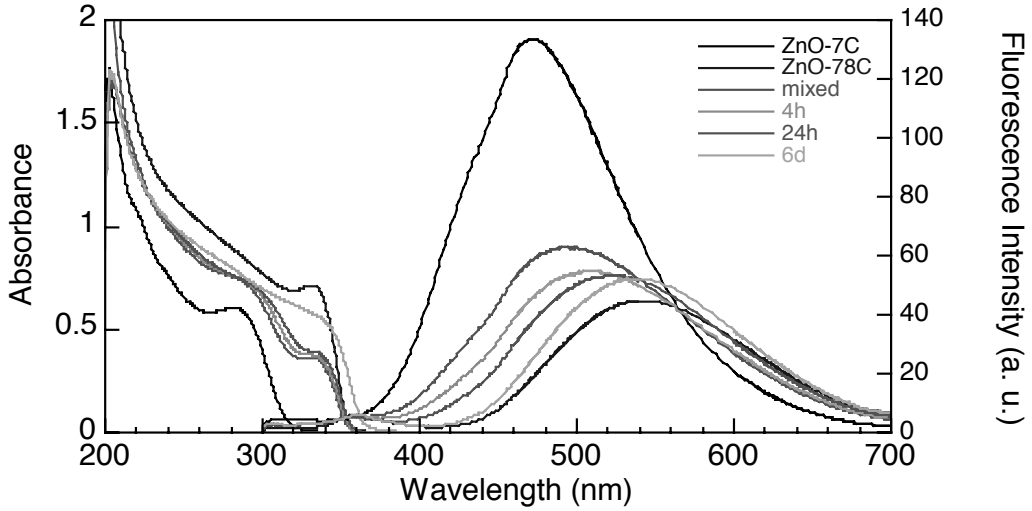


*Fig. 2*: The absorbance and fluorescence spectra of two 1 mM Q-ZnO solutions, made at 7°C (ZnO-7C) and 78°C (ZnO-78C), and combined at time $t = 0$ (mixed), 4 h, 24 h, and 144 h. The exciton absorption band of the smaller particles at 300 nm slowly disappears while the absorption band due to the larger particles grows but does not red-shift. This suggests that after 6 days, the smaller particles have grown significantly, but the larger ones have not, which is consistent with Ostwald ripening in the quantum size regime.

| Solution temperature [°C] | Exciton peak position [nm] | Ave. particle diameter [Å] |
|---|---|---|
| 20 | 288 | 14 |
| 30 | 300 | 18 |
| 40 | 305 | 21 |
| 50 | 309 | 23 |
| 60 | 316 | 27 |
| 70 | 323 | 32 |
| 80 | 322 | 31 |

*Table 1*: The position of the exciton peak for solutions of Q-ZnO made at different temperatures and the average particle size, calculated using the size vs exciton position curve in Figure 5.

| Particle diameter [Å] | Fluorescence FWHM [eV] |
|---|---|
| 9 | 0.70 |
| 14 | 0.57 |
| 18 | 0.58 |
| 24 | 0.53 |
| 34 | 0.64 |

*Table 2*: The particle diameter (determined by XRD peak broadening) vs the fluorescence full width half maximum (FWHM). The width of the trap emission is almost independent of size, suggesting that the surface orbitals are isolated and do not mix with the bulk conduction and valence bands.